

Experimental Evaluation of Synergy-Based In-Hand Manipulation

Gianluca Palli * Fanny Ficuciello ** Umberto Scarcia *
Claudio Melchiorri * Bruno Siciliano **

* DEI - Department of Electrical, Electronic and Information Engineering -
University of Bologna, Viale Risorgimento 2, 40136 Bologna, Italy

** DIETI - Dipartimento di Informatica e Sistemistica, Università degli Studi
di Napoli Federico II, Via Claudio 21, 80125 Napoli, Italy

Abstract: In this paper, the problem of in-hand dexterous manipulation has been addressed on the base of postural synergies analysis. The computation of the synergies subspace able to represent grasp and manipulation tasks as trajectories connecting suitable configuration sets is based on the observation of the human hand behavior. Five subjects are required to reproduce the most natural grasping configuration belonging to the considered grasping taxonomy and the boundary configurations for those grasps that admit internal manipulation. The measurements on the human hand and the reconstruction of the human grasp configurations are obtained using a vision-based mapping method that assume the kinematics of the robotic hand, used for the experiments, as a simplified model of the human hand. The analysis to determine the most suitable set of synergies able to reproduce the selected grasps and the relative allowed internal manipulation has been carried out. The grasping and in-hand manipulation tasks have been reproduced by means of linear interpolation of the boundary configurations in the selected synergies subspace and the results have been experimentally tested on the UB Hand IV.

Keywords: Dexterous Manipulation, Postural Synergies, Robotic Hands, Grasping.

1. INTRODUCTION

Solving the problem of robotic grasping and manipulation involves many complex issues, and the theoretical approach based on the research of optimal solutions results too complex to be implemented in practice with the actual technologies (sensors and computational capability) and poorly reliable due to the simplified modeling of the real system behavior. On the other hand, neuroscience studies point out the natural ability of humans to unconsciously find sub-optimal solutions to those problems. Moreover, the observation of human behavior shows the presence of coordinated motions among the degrees of freedom of the fingers in common to many different grasping postures [Santello et al., 1998, Mason and Salisbury, 1985]. The applications of postural synergies to dexterous robotic hands reported in literature regard essentially problems of hand reshaping during grasping actions and grasp synthesis using the first order synergies, see Ciocarlie and Allen [2009], Wimboeck et al. [2011], Villani et al. [2012]. A synergy-based grasp planning approach relying only on object geometric features and task requirements have being also investigated in literature [Vilaplana and Coronado, 2006, Ficuciello et al., 2012b]. For synergies computation, the Principal Component Analysis (PCA) method has been preferred in several work since it is fast and allows finding global optima with good performance in representing new grasps and, due to its linearity, it allows planning the movements of the robot hand by means of a simple linear interpolation of the synergies [Sun et al., 2010, Wimboeck et al., 2011, Matrone et al., 2010]. At present, the role of synergies in fine manipulation are quite unexplored and the problem of transferring human hand motion to a robotic hand is quite challenging due to the complexity and variety of hand kinematics and the dissimilarity with the robotic hand [Gioioso et al., 2011, Geng et al., 2011]. In this work, we explore the



Fig. 1. Representation of an internal manipulation task starting from a basic grasp posture: from left to right, counter-clockwise rotation, basic grasp and clockwise rotation.

role of synergies in fine manipulation by extending the previous results on grasping. In Ficuciello et al. [2012a] a method based on the acquisition of contact points related to a set of 36 human grasping tasks performed by different test subjects has been described. Since data were collected from subjects with hands that have different kinematics, it was necessary to adopt a normalization procedure to a common kinematic structure which in our case is the UB Hand IV (University of Bologna Hand, version IV) kinematics. Then through kinematic inversion the scaled data were transformed from the Cartesian space to the robotic hand joint space. Finally, the measures have been elaborated by using PCA and the three predominant synergies extracted from the data have been exploited to implement a grasp planner based on defining a trajectory within the synergy subspace. In this work, this previous result is extended in order to represent not only grasps but also manipulation tasks as trajectories connecting suitable configuration sets in the synergy subspace. The basic idea comes out from the observation that there are grasp postures, mainly the precision grasps, that admit internal manipulation (an example is depicted in Fig. 1). Then, starting from the basic reference grasp set, we have enlarged the database of postures by adding the hand configurations that

represents the maximum and minimum bounds for those grasps that admit internal manipulation without loosing the contact between fingertips and the object. To preserve the characteristic and the properties of the previously defined synergy-based grasp synthesis, the in-hand manipulation tasks are represented as deviations from a reference grasp and are obtained by adding so-called manipulation synergies defined in an orthogonal configuration subspace. Preliminary simulations and experimental results are reported to validate the proposed approach.

The paper is organized as follows: Section 2 describes the experimental setup made of 3D vision system for data acquisition and the UB Hand IV. Section 3 describes the method adopted to derive grasp postural synergies and the extension of the synergy-based approach to the manipulation tasks. Section 4 reports the simulation and the experimental evaluation of the proposed synergy-based manipulation planning and, finally, Section 5 provides the conclusion.

2. EXPERIMENTAL SETUP AND DATA ACQUISITION

The kinematics of the UB Hand IV allow the joint angles to be univocally reconstructed from the measurements in 3D space of the fingertip positions. In order to simplify the detection of the human hand postures, a low cost RGBD camera sensor have been used to detect the position of the human fingertips with respect to the wrist. A software application that allows collecting and saving the information coming from the Kinect has been developed, and the data collected in this way have been used for the joint space pose reconstruction by means of an inverse kinematics algorithm. In this way, the occlusion problems that affect motion capture methods for the detection of the human hand postures and joint positions during grasps have been solved.

2.1 Data Acquisition System

The Kinect camera sensor from Microsoft Corp. has been used to provide the RGB color image and the corresponding depth image of the human hand for fingertip position measurements. After a suitable calibration of the device [Zhang and Zhang, 2011], it is possible to reconstruct the 3D real world coordinates (in meters) with respect to the camera frame of each point in the acquired image with precision of about 1.5mm for space and distance in the range of interest of our measurements (an area of about 0.6×0.6 m at a distance of about 0.5 m). This functionality is embedded in the OpenCV library that has been used for the Kinect image elaboration, whereas the freenect driver has been used for low-level communication with the RGBD camera. For the purpose of this work, we developed an application that allows collecting and saving the information coming from the Kinect. The points to be detected are selected by clicking with the mouse on the RGB image and by matching information from the RGB data and depth data.

2.2 The UB Hand IV

The UB Hand IV [Berselli et al., 2009, Palli et al., 2012b] is an innovative anthropomorphic hand developed within the DEX-MART project [DEX]. The hand design aims at an improved human-like manipulation capability and mobility. Indeed, the robotic hand is able to perform the opposition of the thumb with the other four fingers. The Denavit-Hartenberg (DH) parameters of the UB Hand IV are reported in Tab. 1: note that all

Table 1. Denavit-Hartenberg parameters of the UB Hand IV.

Link (Thumb)	d [mm]	θ	a [mm]	α [deg]
1	-42.5	$\theta_1 + 85$	18	-90
2	-1.65	$\theta_2 - 80$	24.57	70.32
3	4.89	$\theta_3 + 10.62$	30	0
4	0	$\theta_4 - 3.61$	30	0
Link (Index)	d [mm]	θ	a [mm]	α [deg]
1	-2.91	θ_1	18	90
2	0	$\theta_2 - 20$	38	0
3	0	θ_3	28	0
4	0	θ_4	28.5	0
Link (middle)	d [mm]	θ	a [mm]	α [deg]
1	-4.91	θ_1	18	90
2	0	θ_2	40	0
3	0	θ_3	28	0
4	0	θ_4	28.5	0
Link (Ring)	d [mm]	θ	a [mm]	α [deg]
1	-1.93	θ_1	18	90
2	0	$\theta_2 - 5$	38	0
3	0	θ_3	28	0
4	0	θ_4	28.5	0
Link (Little)	d [mm]	θ	a [mm]	α [deg]
1	4.24	θ_1	18	90
2	0	$\theta_2 + 15$	35	0
3	0	θ_3	28	0
4	0	θ_4	28.5	0

the fingers present different lengths of the links in order to fit better with the human hand kinematics.

Remotely located actuators with tendon-based transmissions routed by sliding paths [Palli et al., 2012a] have been adopted for the joints actuation. Taking inspiration from the biological model and in order to reduce the complexity of the hand control, an internal non-actuated (passive) tendon has been introduced to couple the movements of the last two joints of each finger, i.e. the medial and the distal joint. Hence, only three angles are considered for the index, the middle, the ring and the little finger, i.e. the base (adduction/abduction) angle θ_{1f} , the proximal angle θ_{2f} and the medial angle θ_{3f} . About the thumb, the angles are: the base (proximal) angle θ_{1t} , the adduction/abduction angle θ_{2t} and the medial angle θ_{3t} . Therefore, a total amount of $h = 15$ joint angles is needed to describe the robotic hand configuration.

3. GRASPS AND MANIPULATION ANALYSIS AND SYNTHESIS

In this section, the synergy-based grasp analysis and synthesis developed in previous works [Ficuciello et al., 2012a] is briefly summarized to provide an overview of the basic grasp planning and the extension of the synergy-based approach to in-hand manipulation tasks representation is reported.

3.1 Synergy-Based Grasp Analysis

The choice of the reference set of postures for grasp synthesis has been made by taking into account the most common human grasp taxonomy reported in literature [Feix et al., 2009, Romero et al., 2010]. The considered set is composed by grasps of objects such as spheres of different dimensions involving a different number of fingers in both power and precise grasp configuration. Cylindrical grasps have been considered as well, distinguishing also between different positions of the thumb. Moreover, several configurations for precise grasps with index



Fig. 2. Reference set of comprehensive human grasps and open-hand configurations used for PCA.

and thumb opposition as well as intermediate side grasps have been included. Furthermore, a discrete number of open-hand configurations with different positions of the thumb and of the adduction/abduction fingers joint has been added in order to find synergies that allow the hand to move continuously also toward open-hand configurations which are equally important to reach and grasp the objects. A total amount of $n = 36$ hand configurations has been considered to derive the fundamental grasp synergies, and a comprehensive hierarchical human grasp classification used for PCA is reported in Fig. 2.

Five human subjects have been asked for reproducing the 36 reference grasps and the measures of the fingertip and palm position have been evaluated using the Kinect camera. The mapping between the human and the robotic hand posture has been performed by assuming the UB Hand IV kinematics as reference model and by scaling the hand dimensions of the 5 subjects to fit the one of the robotic hand. The vector $\mathbf{c}_i \in \mathbb{R}^{15}$ of the joint angle values corresponding to each grasp has been then evaluated by a closed-loop kinematic inversion algorithm and considering the mean value between the measures taken from the 5 subjects. We denoted as $\mathbf{C} = \{\mathbf{c}_i \mid i = 1 \dots n\}$ the matrix of the measurements executed reproducing the reference grasp set. The vector $\bar{\mathbf{c}}$ represents the mean hand position in the grasp configuration space (zero-offset position) and $\mathbf{F} = \{\mathbf{c}_i - \bar{\mathbf{c}} \mid i = 1 \dots n\}$ is the matrix of the grasp offsets with respect to the mean configuration. The PCA has been performed on \mathbf{F} and a base matrix \mathbf{E} of the grasp synergy subspace has been found. The PCA can be performed by diagonalizing the covariance matrix of \mathbf{F} as

$$\mathbf{F}\mathbf{F}^T = \mathbf{E}\mathbf{S}^2\mathbf{E}^T. \quad (1)$$

The 15×15 orthogonal matrix \mathbf{E} gives the directions of variance of the data, and the diagonal matrix \mathbf{S}^2 is the variance in each direction sorted in decreasing magnitude.

3.2 Synergy-Based Grasp Synthesis

Since the three principal components of the matrix \mathbf{E} account for $>85\%$ of the grasp postures, the grasp matrix \mathbf{C} can be reconstructed with good accuracy by adopting the reduced matrix

$$\hat{\mathbf{E}} = [\mathbf{e}_1 \ \mathbf{e}_2 \ \mathbf{e}_3] \quad (2)$$

composed by the three principal components of \mathbf{E} as a base of the robotic hand grasp configuration subspace, thus allowing the control of the robotic hand grasping activities in a configuration space of highly reduced dimensions with respect to the DoF of the hand itself. Each hand grasp \mathbf{c}_i can be approximated by a suitable selection of the synergy coefficients $\alpha_i \in \mathbb{R}^3$

$$\alpha_i = \hat{\mathbf{E}}^\dagger (\mathbf{c}_i - \bar{\mathbf{c}}) \quad (3)$$

where $\hat{\mathbf{E}}^\dagger$ is the Moore-Penrose pseudo-inverse of the base matrix $\hat{\mathbf{E}}$. Therefore, the projection $\hat{\mathbf{c}}_i$ of each robotic hand configuration \mathbf{c}_i on the postural synergies subspace can be evaluated as

$$\hat{\mathbf{c}}_i = \bar{\mathbf{c}} + \hat{\mathbf{E}} \begin{bmatrix} \alpha_{i,1} \\ \alpha_{i,2} \\ \alpha_{i,3} \end{bmatrix} = \bar{\mathbf{c}} + \hat{\mathbf{E}} \alpha_i \quad (4)$$

In the following, the three predominant synergies derived for the UB Hand IV, i.e. the robotic hand motions spanned by \mathbf{e}_1 , \mathbf{e}_2 and \mathbf{e}_3 respectively, are briefly described, referring to the minimum and maximum configuration of each synergy as the hand configurations obtained by means of, respectively, the minimum and maximum value of the corresponding synergy coefficients without violating the joint limits. When the coefficients of the synergies are zero, the hand posture corresponds to the zero-offset position $\bar{\mathbf{c}}$. The vectors of the three synergies and the zero-offset vector of the UB Hand IV are reported in Tab. 2.

First Synergy: With reference to the first postural synergy (column \mathbf{e}_1 in Tab. 2), in the minimum configuration the proximal and medial flexion joint angles of all the fingers are all almost zero and increase their value during the motion toward the maximum configuration. The adduction/abduction movements are not very involved in this synergy.

Table 2. The three predominant synergies and zero offset vectors of the UB Hand IV (in degrees).

		\mathbf{e}_1	\mathbf{e}_2	\mathbf{e}_3	$\bar{\mathbf{c}}[deg]$
Thumb	adduction/abduction	-0.0080	-0.2420	-0.2558	17.76
	proximal	0.0271	0.2665	0.5785	18.8
	medial	0.0615	-0.0003	-0.5136	34.23
Index	adduction/abduction	-0.0387	-0.0109	0.0947	-1.54
	proximal	0.1444	-0.0761	-0.1379	21.9
	medial	0.3145	0.2351	-0.4500	47.89
Middle	adduction/abduction	0.0356	0.0956	0.1184	-1.09
	proximal	0.5016	-0.1457	0.0954	58.7
	medial	0.1901	0.4592	-0.1187	25.79
Ring	adduction/abduction	0.0832	0.0743	0.1453	-0.73
	proximal	0.5293	-0.2752	0.1541	64.69
	medial	0.2032	0.5198	0.0016	26.78
Little	adduction/abduction	0.0677	0.0414	0.1033	-1.24
	proximal	0.4671	-0.2725	0.1120	62.98
	medial	0.1842	0.3650	-0.0209	26.95

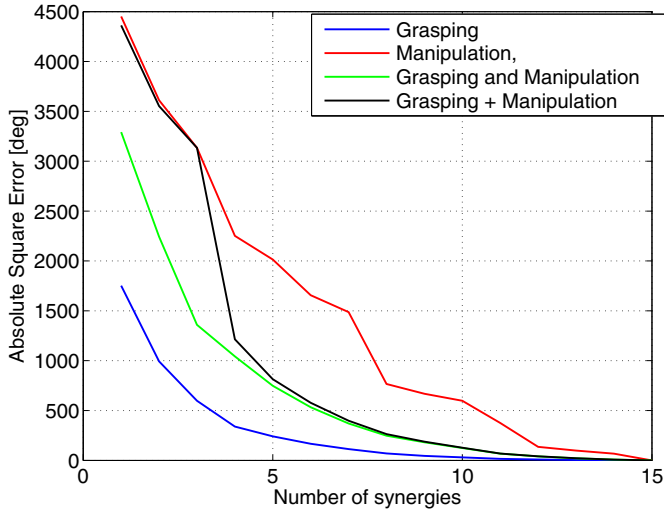


Fig. 3. Absolute square error with respect to the number of synergies.

Second Synergy: The second postural synergy (column \mathbf{e}_2 in Tab. 2) is characterized by a movement in opposite directions of the proximal and medial flexion joints. In this synergy, the adduction/abduction movements of all the fingers are more involved with respect to the first synergy for the index and the little finger.

Third Synergy: In the third postural synergy (column \mathbf{e}_3 in Tab. 2) the movement involves especially the index and the thumb. Thanks to this synergy, the movement of adduction/abduction of the thumb covers the whole joint range without violating other joint limits. This characteristic is crucial because the correct index/thumb opposition allows increasing the grasp accuracy, and thus achieving more stable grasps. This justifies the use of three predominant synergies for the hand control in order to improve the grasp performance. Finally, the excursion of the angles of adduction/abduction of the middle and ring fingers are quite involved in this synergy, more than in the first two.

3.3 Synergy-Based In-Hand Manipulation

For the evaluation of in-hand manipulation tasks, the pad precision grasps shown in Fig. 2 have been used as base postures since they allow the object to be moved with respect to the hand. Then, adopting the same procedure for measuring grasp posture measurement, the same five human subjects have been asked to perform the manipulation tasks, i.e. rotate and translate the object with respect to the palm using the fingers only, and a set of hand postures representing the manipulation task have been recorded. The new hand configuration set $\mathbf{M} = \{\mathbf{c}_{ij} - \bar{\mathbf{c}} \mid i = 1 \dots n, j = 0 \dots m_i\}$ including both the grasp and the manipulation measures is obtained. Note that the vectors \mathbf{c}_{i0} are the previously measured grasp postures, while, for the grasp admitting internal manipulation only, $\mathbf{c}_{ij}, j = 1 \dots m_i$ are the manipulation task configurations associated with the i -th grasp.

For evaluating the effectiveness of synergy-based in-hand manipulation, different approaches can be adopted. The first possible approach is reproducing the hand postures associated to manipulation tasks using the grasp synergies computed on the basis of the grasp reference set shown in Fig. 2. The blue line in Fig. 3 shows the absolute square error obtained by summing

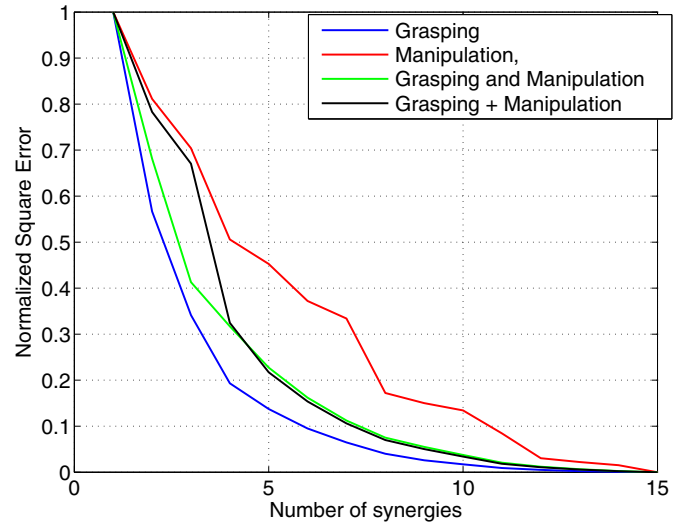


Fig. 4. Normalized square error with respect to the number of synergies.

all the joint error and normalized by the configuration number. Obviously, the error decrease to zero as the number of postural synergies increases. In the same figure, the red line shows the absolute square error in the case the manipulation configuration set is represented by the grasp synergies: the error is significantly larger than in the previous case, showing that the grasp synergies are not suitable to represent manipulation tasks. To improve the quality of the synergy-based manipulations, the synergies can be recomputed using a data set that includes both the grasp configuration set and the manipulation configuration set. The green line in Fig. 3 shows that this solution significantly reduces the absolute square error associated to reproduced configurations. A drawback of this solution is that recomputing all the synergies on the basis of a different data set that includes not only the grasp reference set but also manipulations, completely changes the “shape” of the whole synergy set, and in particular the properties of the first three synergies are not preserved.

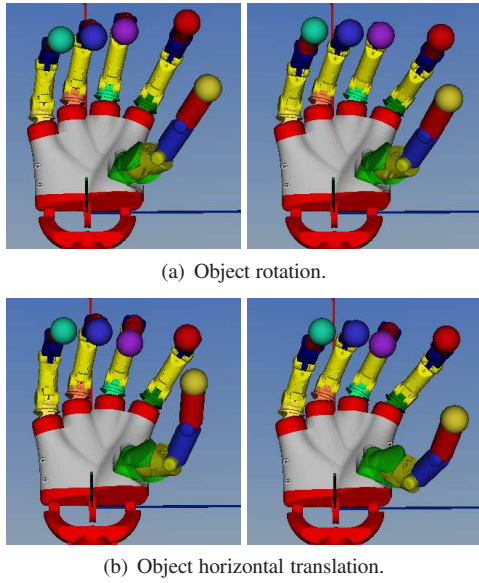
To solve this issue and preserve the properties of the postural synergies computed for grasping, the previous postural synergy base $\hat{\mathbf{E}}$ is selected for the first three synergies, i.e. for grasp synthesis only, then the synergy set is extended including additional synergies, i.e. manipulation synergies, computed using PCA in the subspace of the configuration error by means of the following procedure. Taking into account the whole configuration set, the matrix of the synergy coefficients can be computed as

$$\alpha = \hat{\mathbf{E}}^\dagger \mathbf{M} \quad (5)$$

Note that the coefficient previously computed for reference grasps are preserved. Now, the subspace of the hand configuration error can be found by subtracting from \mathbf{M} the hand configurations projected by using the first three postural synergies:

$$\mathbf{Q} = \mathbf{M} - \hat{\mathbf{E}} \alpha \quad (6)$$

It is important to note that the subspace \mathbf{Q} is orthogonal to the subspace spanned by the first three postural synergies $\hat{\mathbf{E}}$. With the aim of extending the synergy set for correcting the errors with respect to the grasps reference set represented by the base matrix $\hat{\mathbf{E}}$, i.e. for executing of manipulation tasks, a new postural synergy set can be then defined on the space of the configuration error by means of PCA, following the same approach previously adopted in eq. (1):



(a) Object rotation.

(b) Object horizontal translation.

Fig. 5. Simulations of synergy-based manipulation task starting from a five finger precision grasp on a cylindrical object.

$$\mathbf{Q}\mathbf{Q}^T = \mathbf{W}\mathbf{K}^2\mathbf{W}^T. \quad (7)$$

The 15×15 orthogonal matrix \mathbf{W} gives the directions of variance of the error, and the diagonal matrix \mathbf{K}^2 is the variance in each direction sorted in decreasing magnitude. Then, the set of postural synergies used for representing the hand configuration can be enlarged by adding the elements of \mathbf{W}

$$\hat{\mathbf{E}}_{\text{ext}} = [\mathbf{e}_1 \ \mathbf{e}_2 \ \mathbf{e}_3 \ \mathbf{w}_1 \ \mathbf{w}_2 \ \mathbf{w}_3 \ \mathbf{w}_4] = [\hat{\mathbf{E}} \ \hat{\mathbf{W}}] \quad (8)$$

It is worth noticing that four additional manipulation synergies $[\mathbf{w}_1 \ \mathbf{w}_2 \ \mathbf{w}_3 \ \mathbf{w}_4]$ have been introduced in the synergy set since the considered manipulation tasks include four object DoF, i.e. rotation of the object with respect to an axis normal to the palm plane and translation on three orthogonal directions. Given the reference grasp \mathbf{c}_{i0} for a particular manipulation task, the corresponding hand configurations \mathbf{c}_{ij} can be approximated as:

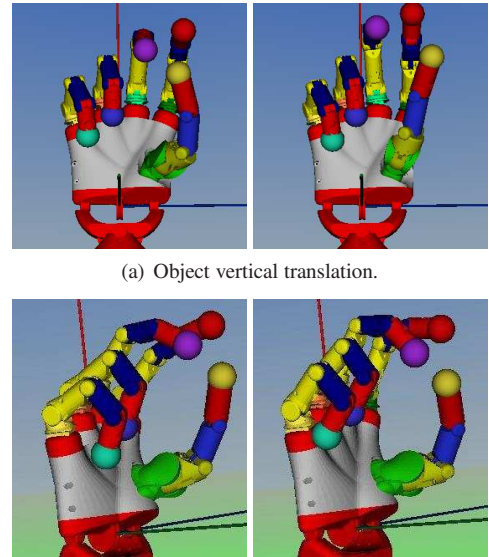
$$\hat{\mathbf{c}}_{ij} = \bar{\mathbf{c}} + \hat{\mathbf{E}}\alpha_i + \hat{\mathbf{W}}\beta_{ij} = \bar{\mathbf{c}} + \hat{\mathbf{E}}_{\text{ext}}[\alpha_i^T \ \beta_{ij}^T] \quad (9)$$

where

$$\beta_{ij} = \hat{\mathbf{W}}^\dagger[\mathbf{c}_{ij} - \hat{\mathbf{c}}_{i0}] \quad (10)$$

This particular selection of the synergy base allows to preserve the properties of the first three postural synergies for what related to grasping tasks, whereas the manipulation tasks can be executed by adding an additional synergy base that is used to correct the corresponding hand posture with respect to the grasp reference posture. An important point to note is that, as shown by the black line in Fig. 3, this selection of the postural synergy base allows, from the point of view of the absolute square error, to obtain the same result as the synergies are computed considering the whole set of hand configurations including both grasp and manipulation tasks.

For a better comparison between the different approaches, the normalized square error of all the cases described above are reported in Fig. 4: from this figure it is possible to note how the error in the representation of the different hand configuration rapidly decreases enlarging the synergy base, restoring the same behavior exhibited in the case the whole synergy set is computed by considering the whole hand configuration set.



(a) Object vertical translation.

(b) Object translation along palm normal direction.

Fig. 6. Simulations of synergy-based manipulation task starting from a tripod precision grasp.

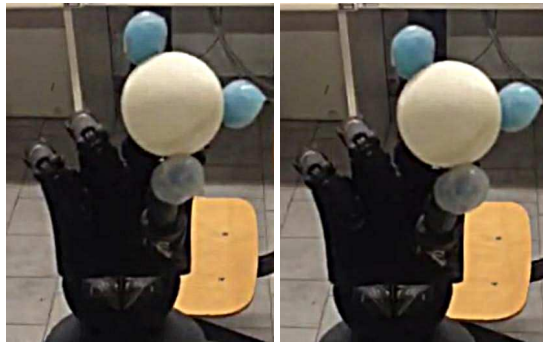
4. SIMULATION AND EXPERIMENTAL EVALUATION OF THE SYNERGY-BASED MANIPULATION

The simulation of all the considered manipulation activities using the Matlab/Simulink environment and VRML for the 3D rendering of the robotic hand motion have been performed to evaluate the ability of the UB Hand IV of reproducing the tasks. Due to space limitations, only few results are here reported. Figure 5 reports the manipulation of a cylindrical object starting from a five finger precision grasp: in Fig. 5(a) the rotation of the object along the palm normal direction is reported, whereas Fig. 5(b) reports the object translation along the horizontal axis. In Fig. 6 the manipulation of a sphere starting from a tripod precision grasp is reported: in Fig. 6(a) the vertical object translation is reported, whereas in Fig. 6(b) the object translation along the palm normal direction is shown.

In the experiments, starting from the basic grasp corresponding to each manipulation task, the hand is moved to by means of the synergy-based approach previously described to perform the manipulation task. Figure 7 reports the experimental evaluation of the manipulation of a spherical object starting from a tripod precision grasp. In particular, Fig. 7(a) reports the rotation of the sphere along the palm normal direction, Fig. 7(b) shows the translation of the object in the horizontal direction and Fig. 7(c) reports the object translation along the vertical direction.

5. CONCLUSION

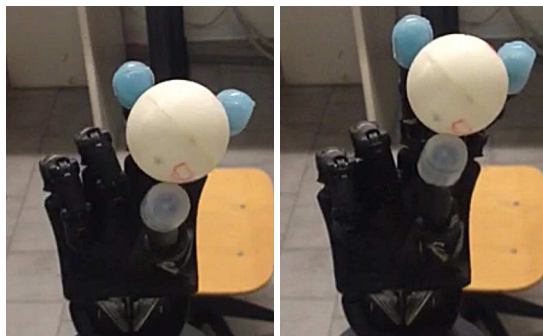
In this paper, a method for describing manipulation task by using postural synergies is reported. The method comprises the measurement of human hand activities using a commercial low-cost RGBD camera such as the Kinect sensor. A closed-loop inverse kinematics algorithm has been used to evaluate the robotic hand configuration by linearly scaling the UB Hand IV kinematics according to the hands dimension of five subjects involved in the experiments and the kinematic patterns of the three predominant grasp synergies of the UB Hand IV have been computed. The synergy-based approach to grasp representation has been then extended to manipulation tasks considering



(a) Object rotation.



(b) Object horizontal translation.



(c) Object vertical translation.

Fig. 7. Experimental evaluation of synergy-based manipulation task starting from a tripod fingertip grasp of a spherical object.

the deviation of the hand configuration during the object motion with respect to the basic grasp posture. An additional set of synergies, called manipulation synergies, has been defined and the manipulation activity reproduced by using this additional synergy set have been evaluated both in simulation and experimentally, showing the effectiveness of the proposed approach in representing simple in-hand manipulations. Future activities will be devoted in verifying the robustness of the approach by performing a wider experimental investigation.

REFERENCES

DEXMART Project website. <http://www.dexmart.eu/>.
G. Berselli, G. Borghesan, M. Brandi, C. Melchiorri, C. Natale, G. Palli, S. Pirozzi, and G. Vassura. Integrated mechatronic design for a new generation of robotic hands. In *Proc. IFAC Symp. on Robot Control*, volume 9, Part 1, pages 105–110, Gifu, Japan, 2009.
Matei T. Ciocarlie and Peter K. Allen. Hand Posture Subspaces for Dexterous Robotic Grasping. *The Int. Journal of Robotics Research*, 28(7):851–867, 2009.

T. Feix, R. Pawlik, H. Schmedmayer, J. Romero, and D. Kragic. The generation of a comprehensive grasp taxonomy. In *Robotics, Science and Systems, Workshop on "Understanding the Human Hand for Advancing Robotic Manipulation"*, Washington, 2009.
F. Ficuciello, G. Palli, C. Melchiorri, and B. Siciliano. Planning and control during reach to grasp using the three predominant UB Hand IV postural synergies. In *Proc. IEEE Int. Conf. Robotics and Automation*, pages 1775–1780, Saint Paul, MN, 2012a.
F. Ficuciello, G. Palli, C. Melchiorri, and B. Siciliano. Postural synergies and neural network for autonomous grasping: a tool for dextrous prosthetic and robotic hands. In *Proc. Int. Conf. on NeuroRehabilitation*, Toledo, Spain, 2012b.
T. Geng, M. Lee, and M. Hulse. Transferring human grasping synergies to a robot. *Mechatronics*, 21(1):272–284, 2011.
G. Gioioso, G. Salvietti, M. Malvezzi, and D. Prattichizzo. Mapping synergies from human to robotic hands with dissimilar kinematics: An object based approach. In *Proc. IEEE Int. Conf. on Robotics and Automation, Workshop on Manipulation Under Uncertainty*, Shanghai, 2011.
M. T. Mason and J. K. Salisbury. *Robot Hands and the Mechanics of Manipulation*. MIT Press, Cambridge, MA, 1985.
G.C. Matrone, C. Cipriani, E.L. Secco, G. Magenes, and M.C. Carrozza. Principal components analysis based control of a multi-dof underactuated prosthetic hand. *Journal of NeuroEngineering and Rehabilitation*, 7(16):1–16, 2010.
G. Palli, G. Borghesan, and C. Melchiorri. Modeling, identification and control of tendon-based actuation systems. *IEEE Trans. on Robotics*, 28(2):277–290, 2012a.
G. Palli, C. Melchiorri, G. Vassura, G. Berselli, S. Pirozzi, C. Natale, G. De Maria, and C. May. *Advanced bimanual manipulation*, chapter Innovative Technologies for the Next Generation of Robotic Hands, pages 173–218. Springer Tracts in Advanced Robotics (STAR). Springer, 2012b.
J. Romero, T. Feix, Hedvig Kjellstrom, and D. Kragic. Spatio-temporal modelling of grasping actions. In *Proc. IEEE/RSJ International Conference on Intelligent Robots and Systems*, pages 2103–2108, Taipei, 2010.
M. Santello, M. Flanders, and J. F. Soechting. Postural hand synergies for tool use. *Journal of Neuroscience*, 18(23):10105–10115, 1998.
S. Sun, C. Rosales, and R. Suarez. Study of coordinated motions of the human hand for robotic applications. In *Proc. Int. Conf. on Information and Automation*, pages 776–781, Harbin, China, 2010.
J.M. Vilaplana and J.L. Coronado. A neural network model for coordination of hand gesture during reach to grasp. *Neural Networks*, 19(1):12–30, 2006.
L. Villani, V. Lippiello, F. Ruggiero, F. Ficuciello, B. Siciliano, and G. Palli. *Advanced bimanual manipulation*, chapter Grasping and Control of Multifingered Hands, pages 219–266. Springer Tracts in Advanced Robotics (STAR). Springer, 2012.
T. Wimboeck, B. Jan, and G. Hirzinger. Synergy-level impedance control for a multifingered hand. In *Proc. Int. Conf. on Intelligent Robots and Systems*, pages 973–979, San Francisco, 2011.
Cha Zhang and Zhengyou Zhang. Calibration between depth and color sensors for commodity depth cameras. In *Proc. Int. Conf. on Multimedia and Expo*, pages 1–6, Barcelona, Spain, 2011.